Liquid Crystals
Publication details, including instructions for authors and subscription information:
http://www.informaworld.com/smpp/title~content=t713926090

Dispersion and attenuation of the eigenwaves for light propagation in heiicoidal liquid crystals

Ibrahim Abdulhalim[a]; Raoul Weil[a]; Lucien Benguigui[a]
[a] Solid State Institute and Department of Physics, Technion-Israel Institute of Technology, Haifa, Israel

To cite this Article Abdulhalim, Ibrahim , Weil, Raoul and Benguigui, Lucien(1986) 'Dispersion and attenuation of the eigenwaves for light propagation in heiicoidal liquid crystals', Liquid Crystals, 1: 2, 155 — 167
To link to this Article: DOI: 10.1080/02678298608086502
URL: http://dx.doi.org/10.1080/02678298608086502

LIQUID CRYSTALS, 1986, VOL. 1, NO. 2, 155–167

Dispersion and attenuation of the eigenwaves for light propagation in helicoidal liquid crystals

by IBRAHIM ABDULHALIM, RAOUL WEIL and LUCIEN BENGUIGUI
Solid State Institute and Department of Physics, Technion–Israel Institute of Technology, 32000, Haifa, Israel

(*Received 29 October 1985; accepted 3 January 1986*)

The dispersion curves and attenuation factors of the Bloch eigenwaves in helicoidal liquid crystals (chiral smectic C and cholesterics) are calculated using the 4×4 characteristic matrix method. Four possible types of eigenmodes are seen to exist in the medium. The reflection peaks, which correspond to odd parts of the full pitch, are total reflection peaks, while those corresponding to even parts of the full pitch are composed of three branches at high incidence angles, where the outer branches are selective reflection and the central one is a total reflection peak. Selective reflection regions occur only at the edges of the Brillouin zones, while total reflections can occur anywhere inside the zones. The former are interpreted according to the coupled mode theory as resonant Bragg reflections, with the latter as exchange Bragg reflections. When the tilt direction exceeds the propagation direction, the central branch of the even sequence of peaks starts to be due to resonant Bragg reflections. The first order peak for cholesterics becomes strongly structured at large incidence angles.

1. Introduction

Bloch eigenwaves are the result of the spatial periodicity of the medium. They have the form of plane waves modulated by a function periodic with the structure. When these waves approach the Brillouin zones' edges, they exhibit reflection toward the adjacent boundary of the Brillouin zone, resulting in an energy gap for the case of electrons in a periodic potential, a stop band for the case of electrical networks and a reflection peak for the case of electromagnetic wave propagation [1, 2]. For the latter case, the helicoidal (chiral smectic C(S_C^*) and cholesteric) liquid-crystalline phases represent a good example for studying light propagation in anisotropic periodic structures. In contrast to the cholesteric case, which has been studied extensively [3–10], only a few investigations have been made [14–18] for the S_C^* case. A review of the optical properties of cholesterics has been given by Belyakov and Dimitrienko [19]; it also includes a section on the optical properties of the S_C^* case using the two-wave approximation of the dynamical theory.

The first study of the eigenmodes for light propagation along the helical axis of cholesterics was given by Nityananda [3, 4]. The two eigenmodes are nearly circularly polarized, where one of them having the same helicity as the medium is reflected from the second Brillouin zone boundary, and the other mode is transmitted without any attenuation.

The properties of the normal waves at oblique incidence has been discussed by Dreher and Meier [5], by evaluating the characteristic exponents of the solutions of the fourth order differential equation. Their charts of stability show the existence of an infinite series of reflection bands, where each band is split into two branches. More recently Saupe and Meier [6] extended this study and found the existence of a triplet of branches. The two outer bands of each triplet give selective reflection of polarized light, while the centre band is unpolarized. The first order reflection peak shows a complicated structure at high incidence angles. The discrepancy with the previous work was attributed to the neglect of one type of the possible eigenmodes. Later, Oldano *et al.* [7] have simplified the infinite determinant of Dreher and Meier [5] to a more analytic form representing the dispersion equation for light propagation in cholesterics. Elachi and Yeh [8] have investigated the problem by finding numerical solutions to the Maxwell equations, in analogy to the solution of the Schrödinger equation for an electron in a periodic potential. Their Brillouin diagram shows that by an appropriate choice of the dielectric constant of the outer isotropic medium and of the angle of incidence, the reflection band may split into two or three bands.

The 4×4 matrix method is a relatively simple, clear and exact method. Shtrickman and Tur [9] first applied it for the computation of the eigenmodes, for the normal incidence case of cholesterics deformed by a magnetic field applied in a direction perpendicular to the helix. More recently Sugita *et al.* [10] applied this method to the general case of cholesterics. Their calculations show the existence of four possible eigenmodes in the medium, where two represent the modes generated at the boundary and the others those reflected from the second boundary. The types of reflection from the cholesteric texture were studied on the basis of a plot of the real and imaginary parts of the wavevectors of the two generated modes at the boundary as a function of the reduced wavelength.

Our present study is devoted mainly to the more general case of the chiral smectic C phase. The cholesteric case is taken as a special case, when the tilt angle equals $\pi/2$. The results are given in graphical form as a function of the tilt and incidence angles for two different values of the outer dielectric constant. Furthermore we give an interpretation to our results according to the coupled mode theory [11–13].

2. Formulation

The 4×4 matrix formulation for light propagation in helicoidal liquid crystals is given by [14]

$$\frac{d\psi}{dz} = \frac{i\omega}{c}\Delta(z)\psi, \tag{1}$$

where $\psi = \begin{pmatrix} E_x \\ H_y \\ -H_x \\ E_y \end{pmatrix}$ and the 4×4 matrix Δ are given in [15]. It has the periodicity p of the structure

$$\Delta(z + p) = \Delta(z). \tag{2}$$

According to the Bloch–Floquet [1, 2] theorem, the solutions to equations (1) and (2) have the form of a plane wave modulated by a function periodic with the structure

$$\psi(z) = u(z)\exp(ikz), \tag{3}$$

where

$$u(z + p) = u(z). \tag{4}$$

Then

$$\psi(z + p) = \exp(ikp)\psi(z). \tag{5}$$

We define the lattice translation operator O_t as

$$O_t z = z + p, \tag{6}$$

applying O_t on $\psi(z)$, we obtain

$$O_t\psi(z) = \psi(O_t^{-1}z) = \psi(z - p). \tag{7}$$

Using equation (3) we find

$$O_t(z)\psi(z) = \exp(-ikp)\psi(z); \tag{8}$$

that is $\exp(-ikp)$ are the eigenvalues of the lattice translation operator, and $\psi(z)$ are its eigenvectors. On the other hand, the characteristic matrix for one period $M(p)$ is defined by [15]

$$\psi(z) = M(p)\psi(z + p). \tag{9}$$

Using equation (5) we find

$$M(p)\psi(z) = \exp(-ikp)\psi(z). \tag{10}$$

Then $\exp(-ikp)$ are also the eigenvalues of the characteristic matrix for one period, and $\psi(z)$ its eigenvectors. The wavevectors k are determined by the secular equation

$$|M(p) - \exp(-ikp)I_4| = 0, \tag{11}$$

where I_4 is the 4×4 unit matrix. This equation gives four values for the wavevector k. Every value of k brings a solution having the form of equation (3) to equation (11). These four solutions are the eigenmodes of the system. Physically, two of them represent the two eigenwaves generated at the first boundary, and the other two represent those reflected from the second boundary.

The calculation of $M(p)$ was described by us [15] recently, using the spiralling dielectric ellipsoid model. Every period of the structure was assumed to consist of 500 molecular layers. The one layer characteristic matrix was calculated using the Lagrange–Sylvester interpolation polynomial. The evaluation of the eigenvalues of $M(p)$ is performed numerically. We are interested in the two eigenmodes generated on the boundary, which have positive imaginary parts of their wavevectors if they are complex, and those which are positive, if they are purely real. Since our calculations were performed as a function of the reduced wavelength, then the graphs present the real and imaginary parts of (kp), not those of k. The real part of (kp) as a function of the reduced wavelength is actually the dispersion curve for that eigenwave. The imaginary part of (kp) represents how much the eigenwave is attenuated in passing through one period, we call it simply the attenuation factor. However, since we have not supposed any dissipation mechanism, the attenuation is due to reflection.

3. Results and discussion

Typical values for the principal dielectric constants were taken [15] $\varepsilon_1 = \varepsilon_2 = 2{\cdot}0$, $\varepsilon_3 = 3{\cdot}0$. The dielectric constant of the outer dielectric semi-infinite media is $\varepsilon_0 = 2{\cdot}3$ in the first case, and for comparison purposes we also take $\varepsilon_0 = 1{\cdot}0$. The number of periods inside the sample is chosen $N = 10$, and each period is divided into $I = 500$ layers.

3.1. *Classification of the eigenwaves*

Let us write $k = k_r + ik_i$, where k_r and k_i are the real and imaginary parts of the wavevectors respectively. Since we are interested in the two modes generated on the $z = 0$ boundary, we have to choose the two modes out of four, which have positive k_r if they are purely real, and positive k_i if they are complex. According to this choice, four possible types of modes are seen to exist:

(1) the two modes are with $k_i = 0$, but $k_r > 0$;
(2) one mode is with $k_i = 0$, but $k_r > 0$, and the other with $k_i > 0$ and $k_r = 0$;
(3) the two modes are with $k_i > 0$ and $k_r = 0$.
(4) the two modes are with $k_i > 0$ and $k_{r_1} = -k_{r_2} \neq 0$.

Type (1) represents two waves propagating without any attenuation. Type (2) represents one reflected eigenwave and the other, a propagating mode without any attenuation. This latter type brings the selective reflection. Type (3) represents two reflected waves, therefore it brings the total reflection. In this latter case, every wave is reflected independently of its polarization state. Type (4) brings also totally reflected waves, but it differs from the usual Bragg reflection (see §4).

According to equation (3), every mode is periodic with k_r, and in order to know its properties, it is usual to investigate it in the interval of one period only. The period is $q_0 = (2\pi/p)$ because

$$\exp(ikp) = \exp\left(i\left(k_r + \frac{2\pi}{p}\right)p\right). \tag{12}$$

The interval chosen originally by Brillouin was between $-\pi/p$ and $+\pi/p$, i.e. $-\pi < k_r p < \pi$. This is the first Brillouin zone known from solid state physics. Every wavevector outside this region could be translated to it by the reciprocal lattice vector translation $G = nq_0$, where n is an integer. Our results are represented in this reduced zone scheme.

3.2. *Incidence angle dependence*

In figures 1 and 2 we show the dependence of the attenuation factors on the incidence angle for the two cases $\varepsilon_0 = 2{\cdot}3$ and $\varepsilon_0 = 1{\cdot}0$, respectively. Actually, there is no difference between the two cases, because the important parameter is the quantity $\sqrt{\varepsilon_0}\sin\phi$ which defines the propagation direction of light inside the medium. In every section of the figures the corresponding dispersion curves for the two eigenwaves can also be seen.

The heights of the attenuation factors for the case with $\varepsilon_0 = 1{\cdot}0$ are lower than those with $\varepsilon_0 = 2{\cdot}3$ (figures 1 (B) and 2 (C)), in correspondence with the results for the reflection peaks calculated in our previous work [15]. We give the explanation to this phenomenon according to the usual Snell's law of refraction. The propagation direction of the wave in the S_c^* medium is closer to the helix in the case with $\varepsilon_0 = 1{\cdot}0$, than that with $\varepsilon_0 = 2{\cdot}3$, and hence the lower height of the reflection. Other differences between these two cases could also be attributed to Snell's law, including the result of Elachi and Yeh [8] concerning the number of branches inside the peak.

At normal incidence, there exists only one unstable region [3] (figure 2 (A)), in which one mode is reflected, hence it is a selective reflection peak of type (2). The real

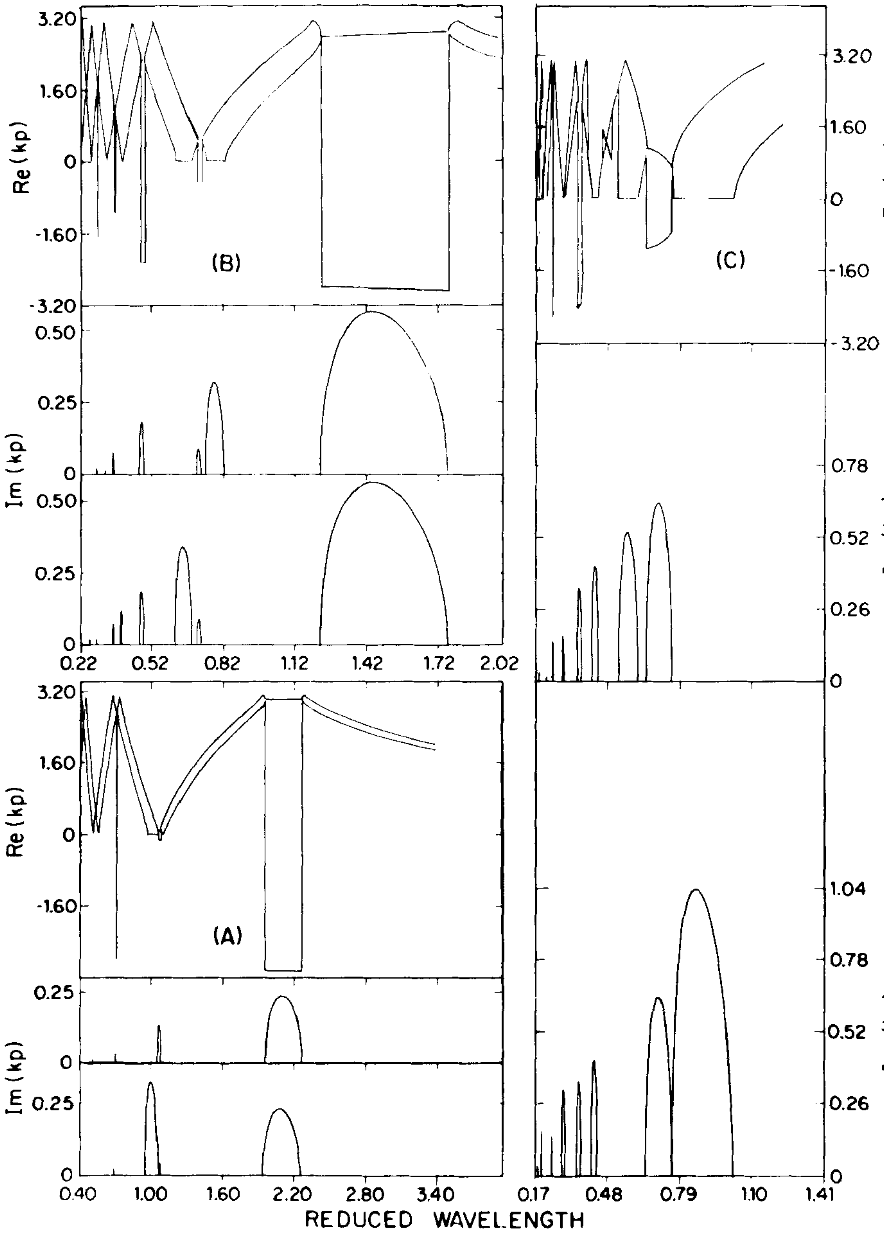

Figure 1. Attenuation factors (imaginary parts) and dispersion curves (real parts) of the two eigenmodes for the case $\varepsilon_0 = 2{\cdot}3$. (A) $\theta = \phi = 45°$, (B) $\theta = 45°$, $\phi = 60°$ and (C) $\theta = 90°$, $\phi = 60°$.

part k_r of the reflected wave is located on the Brillouin zone boundary where the condition is satisfied

$$k_r p = n\pi \tag{13}$$

and $n = 0, \pm 1, \pm 2, \ldots$. The fact that for this case, $n = 0$ indicates that this wavevector is translated by a reciprocal lattice vector from the boundary of another

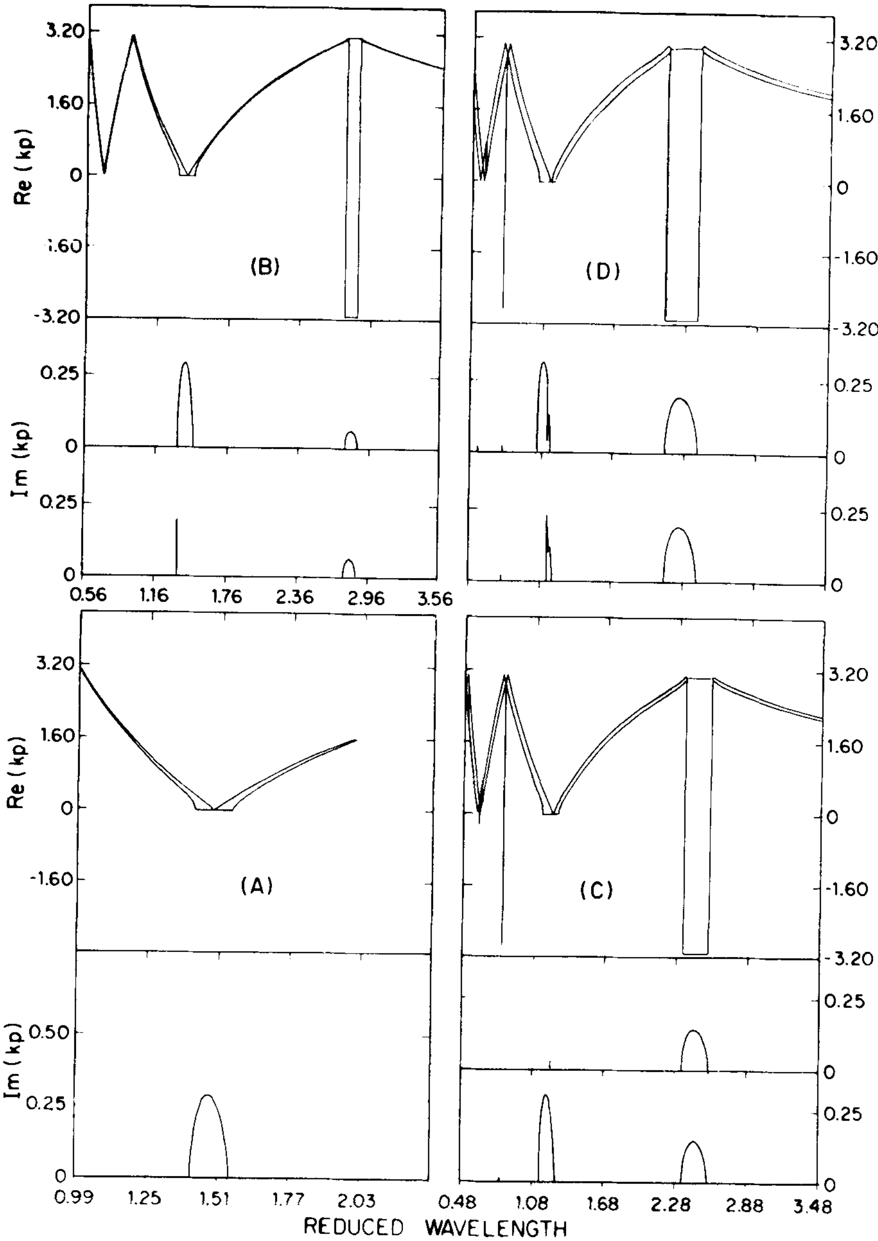

Figure 2. The incidence angle dependence of the attenuation factors and dispersion curves for the case $\varepsilon_0 = 1{\cdot}0$ and fixed tilt angle $\theta = 45°$, (A) $\phi = 0°$, (B) $\phi = 30°$, (C) $\phi = 60°$ and (D) $\phi = 85°$.

Brillouin zone [16]. In this special case it is from the boundary of the second Brillouin zone were $k_r p = \pm 2\pi$, to the first zone, because from the location of this reflection peak, we know it is of second order. The second mode is not reflected from the centre of the gap and its attenuation factor is very close to zero, confirming the analytic solutions given for the normal incidence case [3, 20].

By inclining the propagation direction from the normal, many unstable regions appear. Those are the other Bragg reflection orders. We distinguish between two sequences of peaks; sequence (A) consists of those peaks that correspond to odd parts of the full pitch and it contains the first-order peak, known as the full pitch peak; sequence (B) consists of those that correspond to even parts of the full pitch and it contains the second-order peak known as the half pitch peak.

For the sequence A peaks, the two modes are reflected (type 4) and the real parts of their wavevectors satisfy the condition

$$k_{r_1}p = -k_{r_2}p \simeq \pi. \tag{14}$$

The non-complete equality indicates that this type of reflection is a result of the coupling between the modes, when energy is transferred back and forth between them through the medium. When this occurs, the instability has not to be at the boundary of the Brillouin zone, but everywhere inside it, where the following condition is satisfied:

$$k_{r_1}p + k_{r_2}p = 2\pi m, \tag{15}$$

$m = 0, \pm 1, \pm 2, \ldots$. Such a reflection is called the exchange Bragg reflection according to the formulation of coupled mode theory [13], which we shall discuss in the next section. The heights and widths of the attenuation factors for the sequence A peaks increase monotonically in a saturation behaviour with increasing angle of incidence. There is no splitting after some incidence angle of the first-order peak as we reported recently [15]. This fact indicates that the splitting which we reported was a result of the interaction of this peak with the subsidiary oscillations that came from the boundaries.

Sequence B peaks are more structured, and their dependence on the incidence angle is more complicated. At small incidence angles the two modes are reflected from the centre of the reduced Brillouin zone where one mode is reflected only in a small interval in the centre of the gap. By increasing the incidence angle the appearance of three distinguished regions of instability can be seen (figures 1, 2, 5) inside the gap, where the two outer ones are selective reflections of type (2) and the central one is a total reflection of type (3) or (4). It is of type (3) if the incidence angle is smaller than the tilt angle, and of type (4) if it is greater than or equal to the tilt angle. This result is not the most general, because for the case with $\varepsilon_0 = 1{\cdot}0$ (figure 2) in the whole range of incidence angles, the total reflection region is of type (3). For the cholesteric case (figure 1) it is of type (4). However, ε_0 has the effect of changing the propagation direction inside the medium according to Snell's Law, as mentioned previously. With $\varepsilon_0 = 1{\cdot}0$ and ϕ as large as possible, one obtains a propagation direction closer to the helix axis, than with $\varepsilon_0 = 2{\cdot}3$ and $\phi = 45°$.

According to these results we summarize the phenomenon as follows. In the areas of total reflection for the peaks of sequence B, the condition $k_{r_1}p = -k_{r_2}p \neq 0$ is satisfied. The deviation of $(k_{r_1}p)$ and $(k_{r_2}p)$ from zero depends on ε_0 through the dependence of the propagation direction on ε_0. This deviation becomes clearer when the propagation direction exceeds the tilt direction, and for the cholesteric case, the half pitch peak is strongly structured at large incidence angles. More generally the peaks of total reflection are the result of exchange Bragg reflection and the peaks of selective reflection are the result of direct Bragg reflection [12, 13] where condition (13) is satisfied.

3.3. *Tilt angle dependence*

In figures 3, 4 and 5, the dependence of the attenuation and the dispersion curves on the tilt angle is shown. For the peaks of sequence A the existence of the turning point tilt angle is observed. This angle was mentioned by us recently [15] as the angle where the peaks height and width of the sequence A of peaks start decreasing. A similar tilt angle was reported recently by Oldano [16], where quasi-degeneration occurs and the

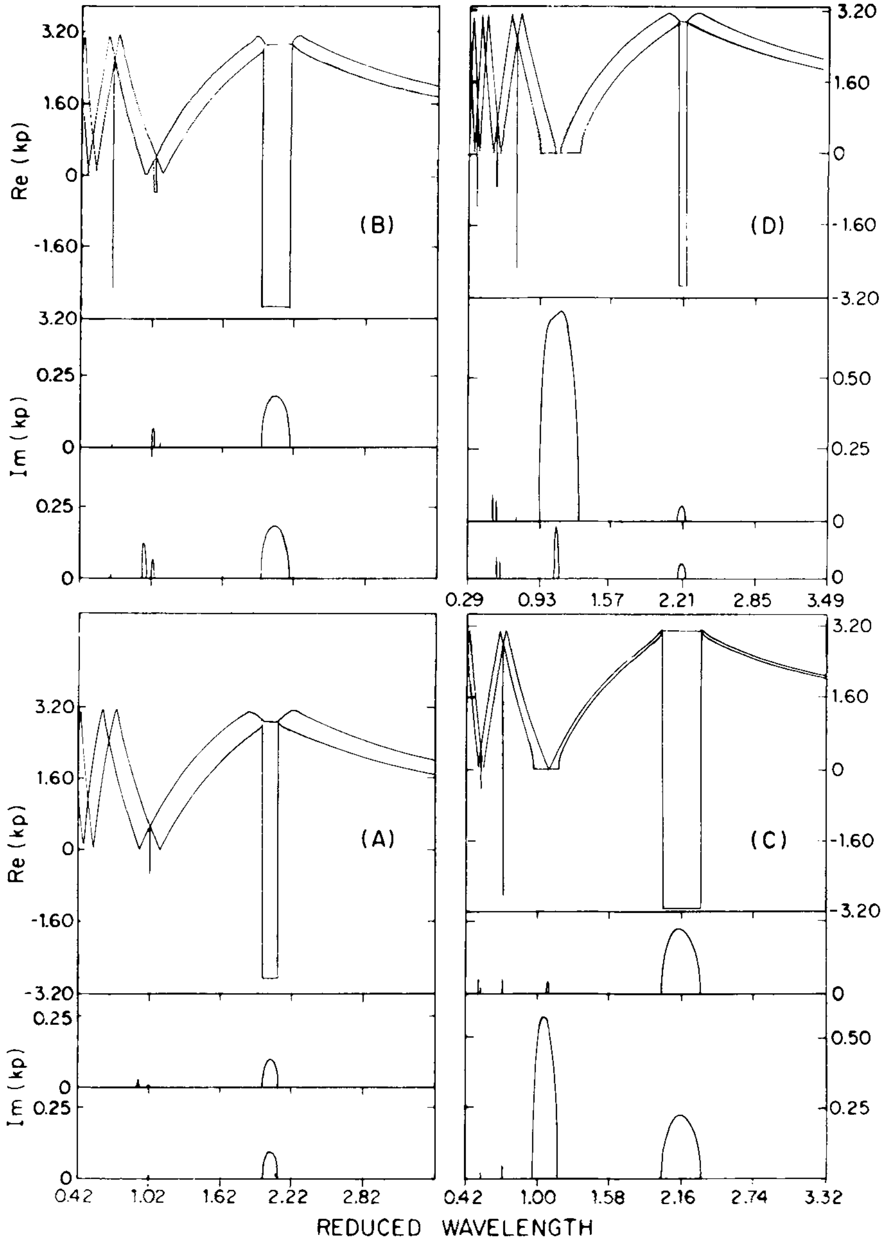

Figure 3. The tilt angle dependence of the attenuation factors and dispersion curves for the case $\varepsilon_0 = 2{\cdot}3$ and fixed incidence angle $\phi = 45°$: (A) $\theta = 15°$, (B) $\theta = 30°$, (C) $\theta = 60°$ and (D) $\theta = 85°$.

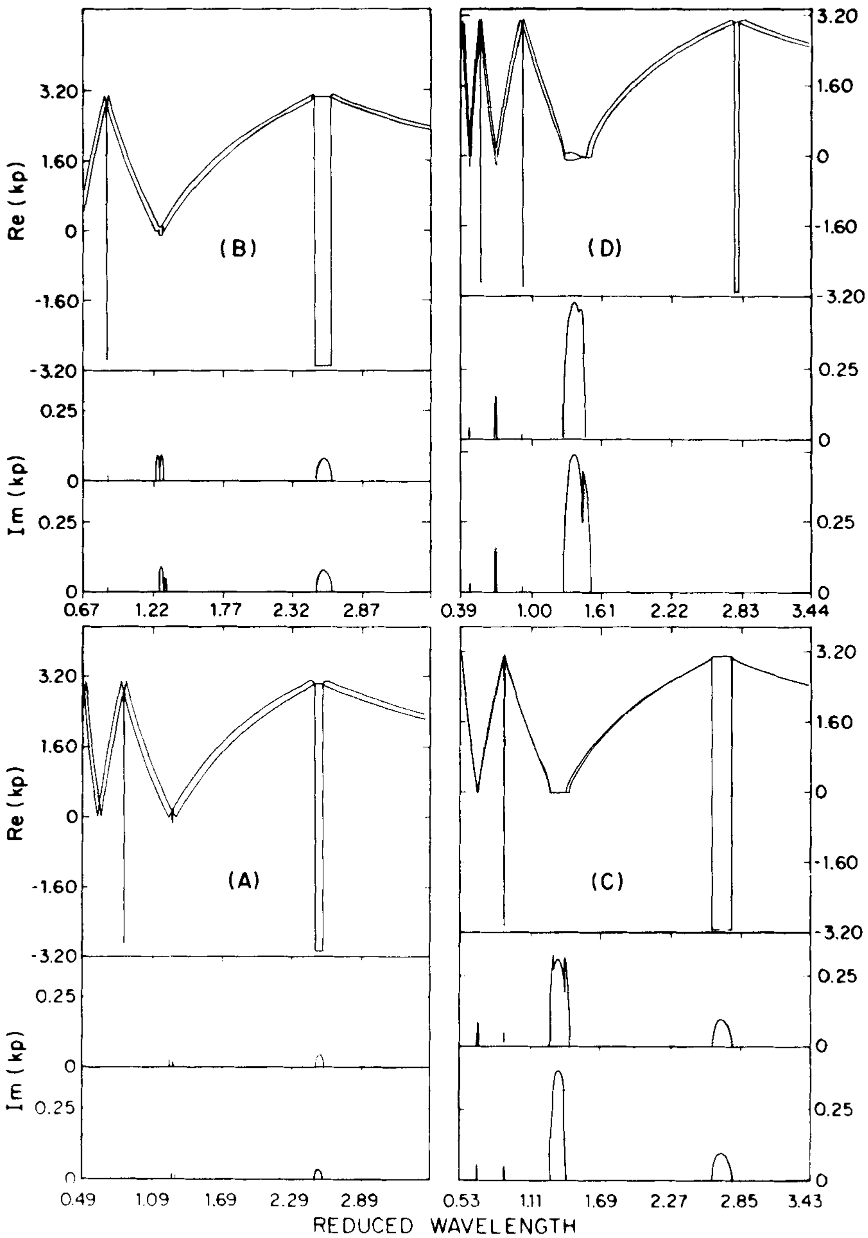

Figure 4. The tilt angle dependence of the attenuation factors and dispersion curves for the case $\varepsilon_0 = 1{\cdot}0$ and fixed incidence angle $\phi = 45°$: (A) $\theta = 15°$, (B) $\theta = 30°$, (C) $\theta = 60°$ and (D) $\theta = 85°$.

polarization states of the eigenfunctions are reversed when passing through such a tilt angle. The quasi-degeneration is also seen in our figures and it occurs near the same tilt angle reported by Oldano (about 56°). However, the quasi-degeneration occurs far from the reflection peaks, while the turning point tilt angle (which is about 51°) is a characteristic of the reflection peak itself. The two critical angles are different, but it

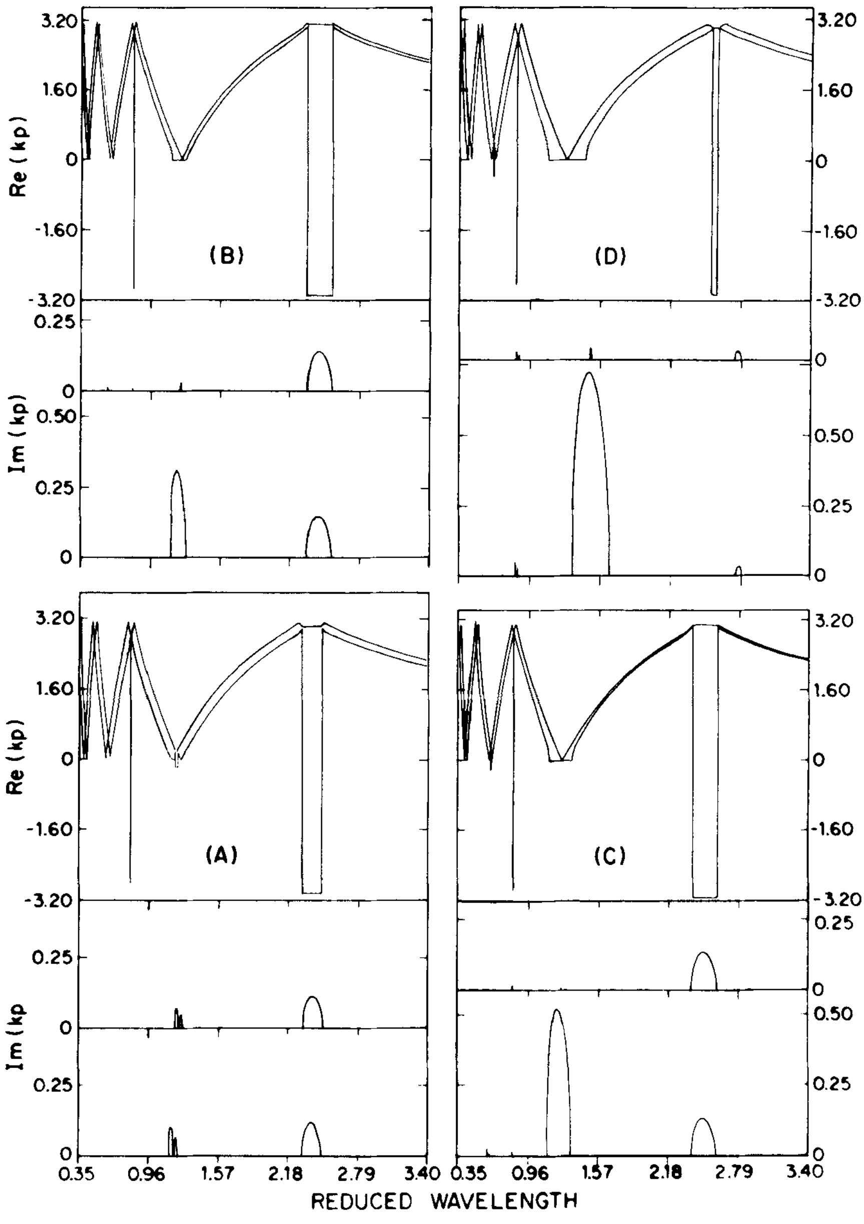

Figure 5. The tilt angle dependence of the attenuation factors and dispersion curves for the case $\varepsilon_0 = 2{\cdot}3$ and fixed incidence angle $\phi = 35°$, (A) $\theta = 30°$, (B) $\theta = 45°$, (C) $\theta = 60°$ and (D) $\theta = 85°$. In (D) a mistake has been discovered after the completion of the manuscript. The curves of Im(kp) have to be shifted to the left, so that the peaks of Im(kp) and Re(kp) coincide with each other.

is not obvious to us, how to connect them. A more detailed study of this subject will appear in a forthcoming paper.

The positions of the peaks of sequence A moves toward the long wavelength region with increasing tilt angle. Sequence B of peaks shows a similar behaviour to that mentioned in the previous section. When the tilt direction is smaller than the propagation direction the half pitch peak is composed of a triplet of bands, where the outer ones are selective reflection bands and the central one is a total reflection band where the modes are of type (4). The deviation of the wavevectors from zero is clearer when the tilt angle is less than the incidence angle; when it is larger, the condition $k_{r_1}p = k_{r_2}p = 0$ is satisfied. The phenomenon is obvious also for the case with $\varepsilon_0 = 1{\cdot}0$ (figure 4).

When the tilt angle is larger than the incidence angle, the structure of the half pitch peak starts to become complicated. For the case with $\varepsilon_0 = 2{\cdot}3$ and $\phi = 35°$ (figure 5), the total reflection region becomes narrower with increasing θ. When $\phi = 45°$ the width for $\theta = 60°$ is less than that for $\theta = 85°$ (cf. figure 3(C)).

For the case $\varepsilon_0 = 1{\cdot}0$, the total reflection region widens with increasing θ. All the peaks become nearly a total reflection region with $k_{r_1}p = k_{r_2}p = 0$, and suddenly when $\theta = 85°$, $k_{r_1}p = -k_{r_2}p \neq 0$ at one-half of the instability region, and the other half is divided into two regions, one with $k_{r_1} = k_{r_2} = 0$, and the other is a selective reflection region.

4. Coupled mode theory interpretation

The coupled mode theory was formulated originally by Kogelnik [11] for thick holograms, and extended by Yariv [12] and Yeh [13] for different cases in optics, including electromagnetic wave propagation in anisotropic media. For the case of a periodic anisotropic medium, the dielectric tensor is written as [12, 13]

$$\boldsymbol{\varepsilon} = \boldsymbol{\varepsilon}_0 + \Delta\boldsymbol{\varepsilon}, \tag{16}$$

where $\boldsymbol{\varepsilon}_0$ is the tensor of the unperturbed medium, and $\Delta\boldsymbol{\varepsilon}$ is the periodic perturbation. The electromagnetic field in the perturbed medium is written as a superposition of four terms, representing the four possible eigenmodes. The four modes could be divided into two sets: two slow modes and two fast modes. Every set represents one forward mode and one backward mode. According to this classification, the four modes are

(i) slow forward mode (sf), with complex amplitude $A(z)$;
(ii) slow backward mode (sb) with complex amplitude $B(z)$;
(iii) fast forward mode (ff) with complex amplitude $C(z)$;
(iv) fast backward mode (fb) with complex amplitude $D(z)$.

The wave form in the medium is the superposition of these four modes. In substituting it into the wave equation we obtain the following results.

(1) *Direct Bragg reflection*

When $k_s p = n\pi$, where $n = 0, \pm 1, \pm 2, \ldots$, and k_s is the wavevector of the slow modes, the following coupled equations are easily obtained:

$$\frac{dA}{dz} = k_{ss}B \quad \text{and} \quad \frac{dB}{dz} = k_{ss}^{*}A; \tag{17}$$

k_{ss} is the coupling constant between the two slow modes. The solution to equation (17) gives that energy is transferred from the slow forward mode (sf) to the slow backward mode (sb). The result is that the incident wave is completely reflected if the interaction region is long enough. Similar equations are obtained for the two fast modes (ff) and (fb) when the condition $k_f p = l\pi$ is satisfied, where k_f is the wavevector of the fast modes and $l = 0, \pm 1, \pm 2, \ldots$. Such reflections are called the direct or resonant Bragg reflections, and occur only on the Brillouin zone boundaries.

(2) *Exchange Bragg reflection*

When the condition $k_s p + k_f p = 2m\pi$ is satisfied, where $m = 0, \pm 1, \pm 2, \ldots$, then the coupling is between the (sf) and (fb) modes or between (sb) and (ff) modes. Physically, energy of one fast (slow) mode is converted to energy of one slow (fast) mode. The result is that the two modes are reflected. This type of reflection is called an exchange Bragg reflection and it could happen anywhere inside the Brillouin zone when this condition is satisfied.

The interesting result from the coupled mode theory is that the coupling constant for the case of direct Bragg reflection depends only on the diagonal elements of the $\Delta\varepsilon$ matrix, while the exchange coupling constant depends only on the off-diagonal elements of the matrix. However, this result has been proved [13, 19] for a special form of the dielectric tensor. We use it here because it offers a physical explanation of our results.

For the case of the S_C^* medium, the dielectric tensor could be expanded in a Fourier series

$$\boldsymbol{\varepsilon} = \sum_{n=-\infty}^{+\infty} \boldsymbol{\varepsilon}_n \exp(inq_0), \tag{18}$$

where

$$\boldsymbol{\varepsilon}_0 = \begin{pmatrix} \frac{\varepsilon_{11}+\varepsilon_{22}}{2} & 0 & 0 \\ 0 & \frac{\varepsilon_{11}+\varepsilon_{22}}{2} & 0 \\ 0 & 0 & \varepsilon_3+\varepsilon_2-\varepsilon_{22} \end{pmatrix}; \quad \boldsymbol{\varepsilon}_{\pm 1} = \frac{\varepsilon_{23}}{2}\begin{pmatrix} 0 & 0 & \pm i \\ 0 & 0 & 1 \\ \pm i & 1 & 0 \end{pmatrix};$$

$$\boldsymbol{\varepsilon}_{\pm 2} = \frac{\varepsilon_{11}-\varepsilon_{22}}{4}\begin{pmatrix} 1 & \mp i & 0 \\ \mp i & -1 & 0 \\ 0 & 0 & 0 \end{pmatrix},$$

and $\boldsymbol{\varepsilon}_n = 0$ for $|n| > 2$. Here ε_1, ε_2, ε_3 are the principal dielectric constants of $\boldsymbol{\varepsilon}$ and $\varepsilon_{11} = \varepsilon_1$, $\varepsilon_{22} = \varepsilon_2 \cos^2\theta + \varepsilon_3 \sin^2\theta$ and $\varepsilon_{23} = -(\varepsilon_3 - \varepsilon_2)\sin\theta\cos\theta$. If we take the zero term $\boldsymbol{\varepsilon}_0$ as the unperturbed part of the dielectric tensor, and the perturbation is $\boldsymbol{\varepsilon}_{\pm 2}$ for the peaks of sequence B and $\boldsymbol{\varepsilon}_{\pm 1}$, for those of sequence A, then we obtain the following results: the tensor $\boldsymbol{\varepsilon}_{\pm 2}$ contains diagonal and off-diagonal elements, so that the peaks of sequence B could be a result of the two types of reflection: the direct and the exchange, in correspondence to what we get for this sequence of peaks. On the other hand, the tensor $\boldsymbol{\varepsilon}_{\pm 1}$ contains only off-diagonal elements, so that the peaks of sequence A result only from exchange Bragg reflection as we mentioned in §3. For the cholesteric case, however, the term $\boldsymbol{\varepsilon}_{\pm 1}$ does not exist, and so the peaks of sequence A also do not exist either.

5. Conclusions

In this work we have presented results of calculations of the dispersion and attenuation of the Bloch eigenwaves that exist in S_C^* and cholesteric media. The computations were based on the 4×4 characteristic matrix method, where the wavevectors are obtained by diagonalizing the one period characteristic matrix, and hence four possible types of eigenmodes exist in the medium.

The sequence of the reflection peaks which correspond to odd parts of the full pitch, are total reflections and interpreted according to the coupled mode theory as exchange Bragg reflections where coupling between the fast and slow modes occur. The reflection peaks which correspond to even parts of the full pitch are composed of three branches at high incidence angles, where the outer branches are selective reflections and the central branch is a total reflection peak. This composition of the latter sequence of peaks is interpreted according to the coupled mode theory as a result of the existence of both diagonal and off-diagonal elements in the matrix of the second order Fourier coefficient of the dielectric tensor. The diagonal elements give the selective reflection where the Bragg condition $k_{r_1}p = n\pi$ is satisfied and hence they are called direct Bragg reflection, where they occur only on the Brillouin zone boundary. The off-diagonal elements give the total reflection peaks where the condition $k_{r_1}p + k_r p = m\pi$ is satisfied and hence they are called exchange Bragg reflections, where they can occur anywhere inside the Brillouin zone.

The dependence of the curves on the tilt and incident angles was evaluated for two different values of the outer dielectric constant. When the tilt angle exceeds the propagation angle with respect to the helix axis, the central branch of the even sequence of peaks starts to be due to resonant Bragg reflections. The odd sequence of peaks does not exist in the cholesteric case, because the first order Fourier coefficient of the dielectric tensor vanishes. In this case the first peak of the even sequence becomes strongly structured at high incidence angles.

References

[1] Kittel, C., 1967, *Introduction to Solid State Physics*, 3rd edition (Wiley), p. 63.
[2] Brillouin, L., 1953, *Wave Propagation in Periodic Structures* (Dover), p. 139.
[3] Nityananda, R., 1973, *Molec. Crystals liq. Crystals*, **21**, 315.
[4] de Gennes, P. G., 1974, *The Physics of Liquid Crystals* (Oxford University Press).
[5] Dreher, R., and Meier, G., 1973, *Phys. Rev.* A, **8**, 1616.
[6] Saupe, A., and Meier, G., 1983, *Phys. Rev.* A, **27**, 2196.
[7] Oldano, C., Miraldi, E., and Taverna Valabrega, P., 1983, *Phys. Rev.* A, **27**, 3291.
[8] Elachi, C., and Yeh, C., 1974, *J. opt. Soc. Am.*, **64**, 1178.
[9] Shtrickman, S., and Tur, M., 1974, *J. opt. Soc. Am.*, **64**, 1178.
[10] Sugita, A., Takezoe, H., Ouchi, Y., Fukuda, A., Kuze, E., and Goto, N., 1982, *Jap. J. appl. Phys.*, **21**, 1543.
[11] Kogelnik, H., 1969, *Bell Syst. tech. J.*, **48**, 2909.
[12] Yariv, A., 1973, *I.E.E.E. Jl quant. Electron*, **9**, 919.
[13] Yeh, P., 1979, *J. opt. Soc. Am.*, **69**, 742.
[14] Berreman, D. W., 1973, *Molec. Crystals liq. Crystals*, **22**, 175.
[15] Abdulhalim, I., Benguigui, L., and Weil, R., 1985, *J. Phys., Paris*, **46**, 815.
[16] Oldano, C., 1984, *Phys. Rev. Lett.*, **53**, 4313.
[17] Oldano, C., Allia, P., and Trossi, L., 1985, *J. Phys., Paris*, **46**, 573.
[18] Taupin, D., Guyon, E., and Pieranski, P., 1978, *J. Phys., Paris*, **39**, 406.
[19] Belyakov, V., Dimitrienko, V. E., and Orlov, V. P., 1979, *Soviet Phys. Usp.*, **22**, 63.
[20] Parodi, P., 1975, *J. Phys., Paris*, C1, **36**, 22.